

Palladium-Allyl Phosphoramidite Complexes: Solid-State Structures and Solution Dynamics

Serena Filipuzzi and Paul S. Pregosin*

Laboratory of Inorganic Chemistry, ETH HCI, Hönggerberg CH-8093 Zürich, Switzerland

Alberto Albinati* and Silvia Rizzato

Department of Structural Chemistry (DCSSI), University of Milan, 20133 Milan, Italy

Received August 9, 2006

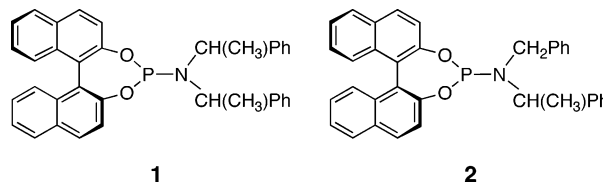
Several mono-phosphoramidite and bis-phosphoramidite 2-methylallyl and 1,3-diphenylallyl allyl complexes of Pd(II) have been prepared. The solid-state structure for one of these has been determined. The mono-phosphoramidite chloro-allyl complexes of Pd(II) exist in two isomeric forms in solution. ^1H , ^1H NMR exchange spectroscopy reveals that the dinuclear species $[\text{Pd}(\mu\text{-Cl})(\eta^3\text{-CH}_2\text{C}(\text{Me})\text{CH}_2)]_2$ is involved in the interconversion between the two isomers. There is evidence to suggest that phosphoramidite dissociation is not responsible for this exchange. The cationic η^3 -2-methylallyl bis-phosphoramidite Pd complexes reveal *nonequivalent* ^{31}P resonances, as a consequence of slow allyl dynamics and in agreement with the preliminary X-ray structure.

Introduction

There is an increasing interest in monodentate chiral auxiliaries. Although the 1,1'-(2-diphenylphosphino)binaphthyl, MOP, class, initiated by Hayashi,¹ has been quite successful, current interest has centered on binol-based phosphite² and phosphoramidite ligands.³ The chiral phosphoramidite class of ligands has found applications in Rh(I)-catalyzed asymmetric hydrogenation,^{4a} e.g., of β -(acylamino)acrylates,^{4b} rhodium-catalyzed asymmetric conjugate additions of boronic acids,^{4c} ruthenium-catalyzed oxidation,⁵ copper-catalyzed C–C bond making,⁶ asymmetric intramolecular Heck reactions,⁷ asymmetric palladium-catalyzed hydrosilylation,⁸ and palladium-catalyzed allylic alkylation reactions,⁹ to name just a few. Occasionally, a coordinated phosphoramidite ligand can function as a bidentate ligand.¹⁰

Increasingly the α -phenethyl phosphoramidite derivative, **1**, is employed, as this provides additional stereogenic centers;

however, a number of related compounds, e.g., **2**, are also in use. Clearly, given the modestly complicated nature of these

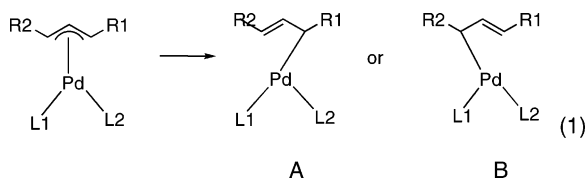


ligands, both the P-donor strength and the steric bulk of **1** and **2** are likely to affect proximate coordinated ligands and substrates.

It is now recognized^{11–19} that an η^3 - π allyl complex can isomerize to its η^1 - σ -allyl counterpart; see eq 1. There are a number

- (1) Hayashi, T. *Acc. Chem. Res.* **2000**, *33*, 354–362.
 (2) Reetz, M. T.; Mehler, G.; Bondarev, O. *Chem. Commun.* **2006**, 2292–2294. Reetz, M. T.; Li, X. G. *J. Am. Chem. Soc.* **2006**, *128*, 1044–1045. Reetz, M. T.; Ma, J. A.; Goddard, R. *Angew. Chem., Int. Ed.* **2005**, *44*, 412–415. Reetz, M. T.; Mehler, G.; Meiswinkel, A. *Tetrahedron: Asymmetry* **2004**, *15*, 2165–2167. Reetz, M. T.; Sell, T.; Meiswinkel, A.; Mehler, G. *Angew. Chem., Int. Ed.* **2003**, *42*, 790–793.
 (3) Feringa, B. L. *Acc. Chem. Res.* **2000**, *33*, 346.
 (4) (a) Peña, D.; Minnaard, A. J.; de Vries, J. G.; Feringa, B. L. *J. Am. Chem. Soc.* **2002**, *124*, 14552–14553. (b) Hu, X. P.; Zhuo, Z. *Org. Lett.* **2005**, *7*, 419–422. (c) Martina, S. L. X.; Minnaard, A. J.; Hessen, B.; Feringa, B. L. *Tetrahedron Lett.* **2005**, *46*, 7159–7163.
 (5) Huber, D.; Mezzetti, A. *Tetrahedron: Asymmetry* **2004**, *15*, 2193–2197.
 (6) Naasz, R.; Arnold, A. L.; Pineschi, M.; Keller, E.; Feringa, B. L. *J. Am. Chem. Soc.* **1999**, *121*, 1104–1105. de Vries, A. H. M.; Meetsma, A.; Feringa, B. L. *Angew. Chem.* **1996**, *108*, 2526. van Zijl, A. W.; Arnold, L. A.; Minnaard, A. J.; Feringa, B. L. *Adv. Synth. Catal.* **2004**, *346*, 413–420.
 (7) Imbos, R.; Minnaard, A. J.; Feringa, B. L. *Dalton Trans.* **2003**, 2017–2023.
 (8) Guo, X. X.; Xie, J. H.; Hou, G. H.; Shi, W. H.; Wang, L. X.; Zhou, Q. L. *Tetrahedron: Asymmetry* **2004**, *15*, 2231–2234.
 (9) Boele, M. D. K.; Kamer, P. C. J.; Lutz, M.; Spek, A. L.; de Vries, J. G.; van Leeuwen, P.; van Strijdonck, G. P. E. *Chem.–Eur. J.* **2004**, *10*, 6232–6246. Zononi, G.; Gladiali, S.; Marchetti, A.; Piccinini, P.; Tredici, I.; Vidari, G. *Angew. Chem., Int. Ed.* **2004**, *43*, 846–849.

- (10) Huber, D.; Kumar, P. G. A.; Pregosin, P. S.; Mezzetti, A. *Organometallics* **2005**, *24*, 5221–5223.
 (11) Vrieze, K. Fluxional Allyl Complexes. In *Dynamic Nuclear Magnetic Resonance Spectroscopy*; Jackman, L. M., Cotton, F. A., Ed.; Academic Press: New York, 1975; pp 441–483.
 (12) Pregosin, P. S.; Salzmänn, R. *Coord. Chem. Rev.* **1996**, *155*, 35–68. Herrmann, J.; Pregosin, P. S.; Salzmänn, R.; Albinati, A. *Organometallics* **1995**, *14*, 3311. Pregosin, P. S.; Salzmänn, R.; Togni, A. *Organometallics* **1995**, *14*, 842–847.
 (13) Breutel, C.; Pregosin, P. S.; Salzmänn, R.; Togni, A. *J. Am. Chem. Soc.* **1994**, *116*, 4067. Burckhardt, U.; Gramlich, V.; Hofmann, P.; Nesper, R.; Pregosin, P. S.; Salzmänn, R.; Togni, A. *Organometallics* **1996**, *15*, 3496–3503. Togni, A.; Burckhardt, U.; Gramlich, V.; Pregosin, P.; Salzmänn, R. *J. Am. Chem. Soc.* **1996**, *118*, 1031–1037.
 (14) Cesarotti, E.; Grassi, M.; Prati, L.; Demartin, F. *J. Organomet. Chem.* **1989**, *370*, 407–419. Cesarotti, E.; Grassi, M.; Prati, L.; Demartin, F. *J. Chem. Soc., Dalton Trans.* **1991**, 2073. Mandal, S. K.; Gowda, G. A. N.; Krishnamurthy, S. S.; Zheng, C.; Li, S. J.; Hosmane, N. S. *Eur. J. Inorg. Chem.* **2002**, 2047–2056. Mandal, S. K.; Gowda, G. A. N.; Krishnamurthy, S. S.; Zheng, C.; Li, S. J.; Hosmane, N. S. *J. Organomet. Chem.* **2003**, *676*, 22–37. Mandal, S. K.; Gowda, G. A. N.; Krishnamurthy, S. S.; Nethaji, M. *Dalton Trans.* **2003**, 1016–1027.
 (15) Crociani, B.; Antonaroli, S.; Paci, M.; Di Bianca, F.; Canovese, L. *Organometallics* **1997**, *16*, 384–391. Crociani, B.; Antonaroli, S.; Bandoli, G.; Canovese, L.; Visentin, F.; Uguagliati, P. *Organometallics* **1999**, *18*, 1137–1147.
 (16) Gogoll, A.; Ornebro, J.; Grennberg, H.; Bäckvall, J. E. *J. Am. Chem. Soc.* **1994**, *116*, 3631.
 (17) Sprinz, J.; Kiefer, M.; Helmchen, G.; Reggelein, M.; Huttner, G.; Zsolnai, L. *Tetrahedron Lett.* **1994**, *35*, 1523–1526. Kollmar, M.; Helmchen, G. *Organometallics* **2002**, *21*, 4771–4775.

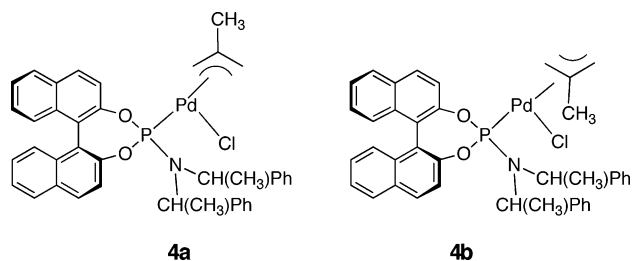


of subsequent mechanistic steps that may accompany this isomerization, e.g., rotation around either the Pd–C or the allyl C–C bond. We have had a long-standing interest in the structures and dynamics of chiral Pd-allyl complexes.^{12,13} Specifically, we have shown that the nature of the chiral auxiliary markedly affects the isomerization dynamics associated with the allyl ligand.¹² The η^3 – η^1 allyl isomerization can be either under electronic control (the strongest donor labilizes the terminal allyl carbon in pseudo-*trans* position) or under steric control (the largest ligand induces opening of the *cis*-positioned terminal allyl carbon).^{12,13} Consequently, the formation of either structure A or B will depend strongly on the characteristics of the ligands L1 and L2.

To determine how the phosphoramidite ligands **1** and **2** affect this type of isomerization, we have prepared the 2-methallyl complexes **4** and **5**, from **3**, and the 1,3-diphenylallyl compounds **7** and **8**, from **6**; see Scheme 1. Further, we have synthesized the 2-methallyl bis-phosphoramidite salts, **9**–**11**. We report here aspects of the solid-state and solution structures for these palladium complexes and comment on the mechanism(s) of their isomerization reactions, via 2-D phase-sensitive ¹H NOESY NMR spectra.

Results and Discussion

The allyl chloro complexes, **4**, **5**, **7**, and **8**, are readily prepared from the halogen-bridged complexes, **3** and **6**, by addition of 2 equiv of the ligand per dimer. These allyl complexes exist in two isomeric forms in dichloromethane solution. The isomers stem from the relative positions of the allyl ligands with respect to the substituents on the P atom, e.g., **4a** and **4b**. Since we do



not find *interligand* NOEs between the allyl and the P-donor, we cannot assign the NMR signals to any one particular isomeric structure.

The bis-phosphoramidite salts **9**–**11** (complex **11** contains the dimethylamino analogue, “monophos”; see Scheme 1) were prepared from **3**, via addition of 2 equiv of AgBF₄ and 4 equiv of the phosphoramidite, in dichloromethane solution, as indicated in eq 2.

X-ray Studies. Figure 1 shows an ORTEP view of the neutral complex **4**, and Table 1 gives a list of selected bond lengths and bond angles for this species. For **4**, where one finds two

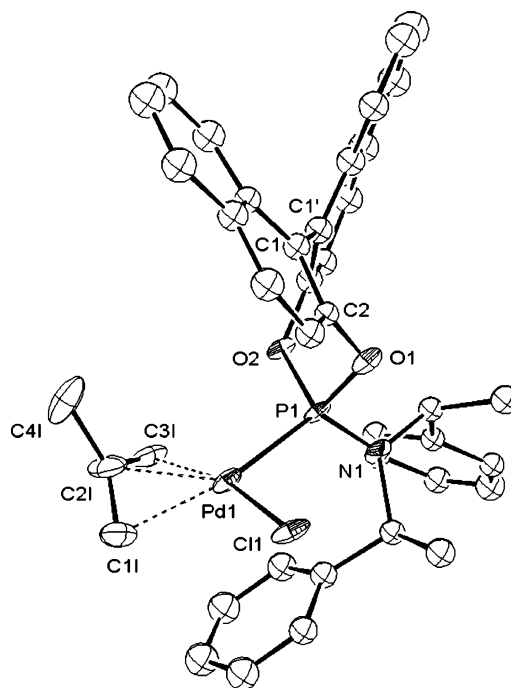
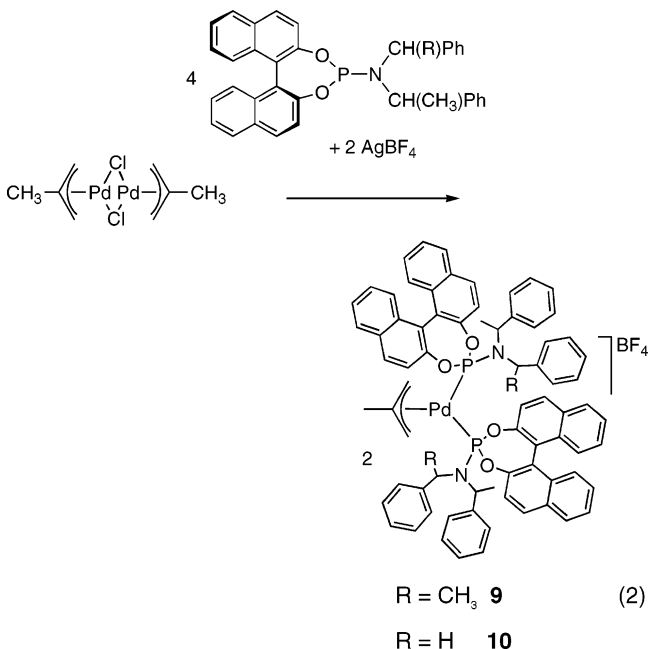


Figure 1. ORTEP view of the neutral Pd complex **4**.

nonequivalent molecules in the unit cell, the immediate coordination sphere consists of the η^3 -allyl ligand, the chloride, and the P atom of the phosphoramidite. The two bis α -phenethyl moieties are proximate to the Cl atom, whereas the bis-naphthyl fragment is situated above the Pd atom on the same side as the allyl methyl group.

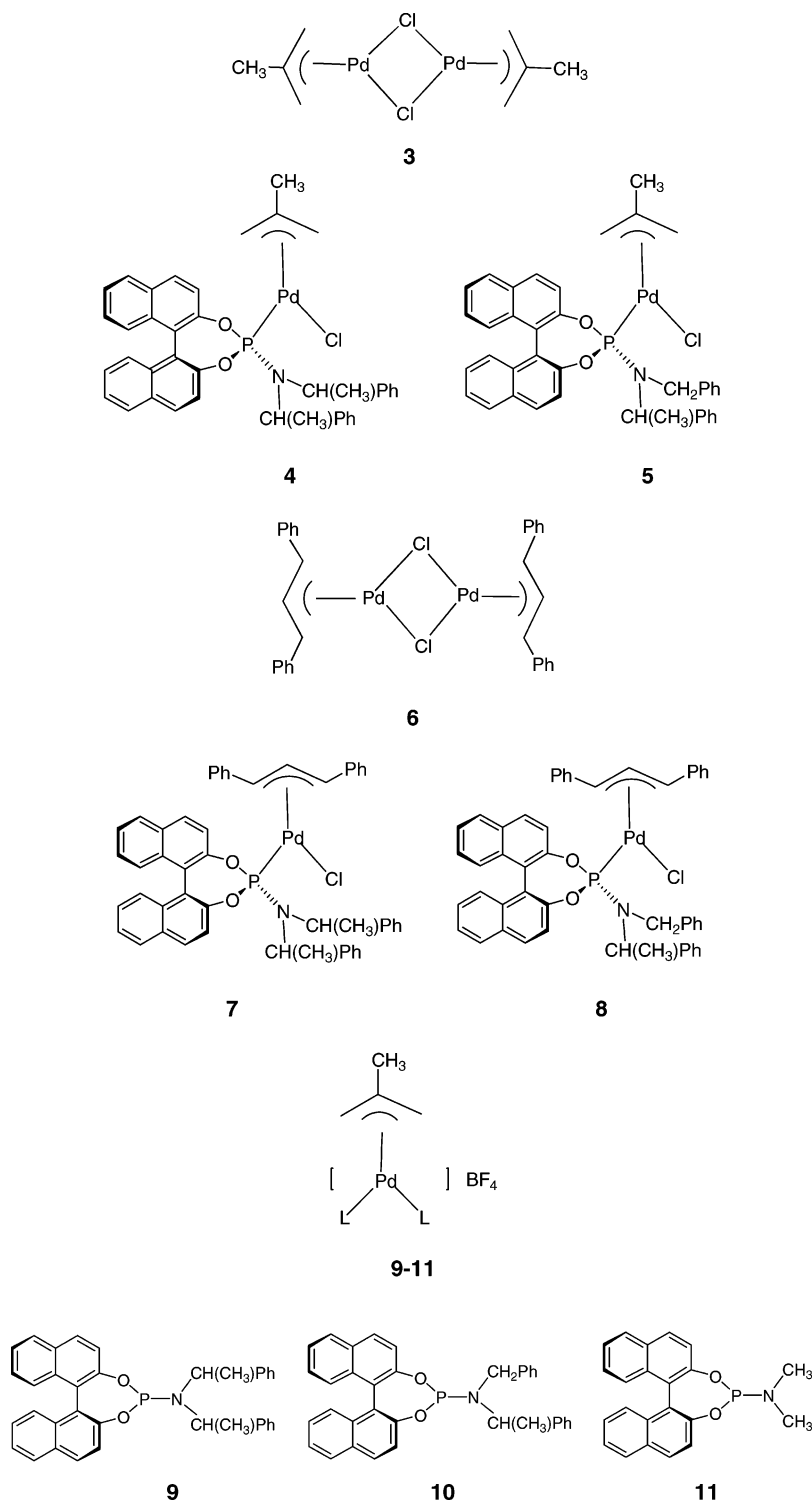


The solid-state structure for **9** (where there are also two nonequivalent molecules in the unit cell) proved difficult to refine satisfactorily due to the poor quality of the crystals, the disorder arising from water molecules and the solvent dichloromethane. Nevertheless, there is no question as to the overall structure of the cation, and we show this in Figure 2. The immediate coordination sphere is made up of the two phosphoramidite P atoms and the η^3 -allyl ligand. In terms of the structure of the chiral pocket, for **9**, it is interesting to note that

(18) Faller, J. W.; Wilt, J. C. *Organometallics* **2005**, *24*, 5076–5083.
Faller, J. W.; Sarantopoulos, N. *Organometallics* **2004**, *23*, 2179–2185.
Faller, J. W.; Wilt, J. C.; Parr, J. O. *Org. Lett.* **2004**, *6*, 1301–1304.
Faller, J. W.; Stokes-Huby, H. L.; Albrizzio, M. A. *Helv. Chim. Acta* **2001**, *84*, 3031–3042.

(19) Lloyd-Jones, G. C.; Stephen, S. C.; Murray, M.; Butts, C. P.; Vyskocil, S.; Kocovsky, P. *Chem. Eur. J.* **2000**, *6*, 4348–4357.

Scheme 1



the terminal allyl carbon C11L is proximate to an α -phenethyl group, whereas the other terminal allyl carbon, C13L, is proximate to a naphthyl group. If this difference were maintained in solution, it would explain the observed nonequivalent ^{31}P resonances for the phosphoramidite ligands of **9** and **10** in solution (*vide infra*).

Table 1 also gives X-ray data from several known^{20–22} model palladium allyl complexes, **12–14**. If one uses the Pd–C(allyl) separations as an indication of the *trans* influence of the phos-

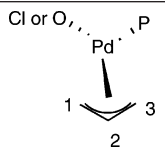
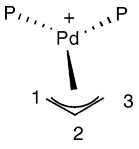
phoramidite P-donor, it can be seen that, on the basis of a comparison of **4** with **13**, the phosphoramidite ligands are not very different, but perhaps slightly weaker than the PCy_3 ligand in **14**. The Pd–C1 bond length is ca. 2.18 Å in both compounds. There are a number of known structures of bis-P-donor allyl palladium complexes, e.g., **15–17** (also shown in the table), and the Pd–C(allyl) separations do not seem to vary a great

(21) Boele, M. D. K.; Kamer, P. C. J.; Lutz, M.; Spek, A. L.; de Vries, J. G.; van Leeuwen, P. W. N. M.; van Strijdonck, G. P. F. *Chem. Eur. J.* **2004**, *10* (24), 6232.

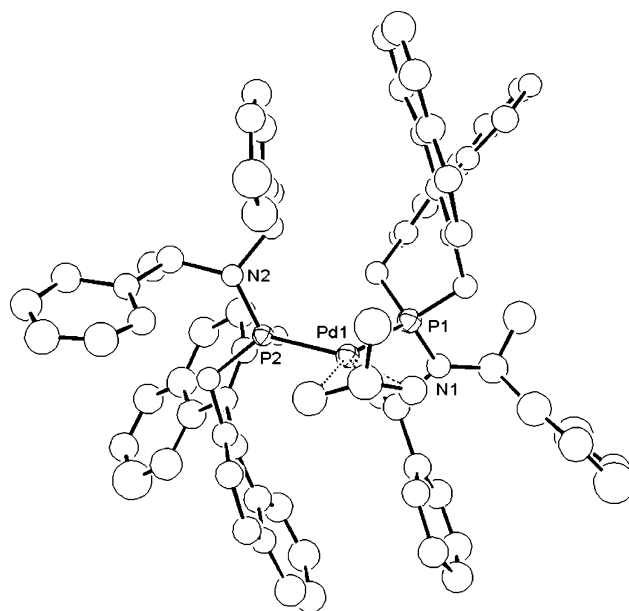
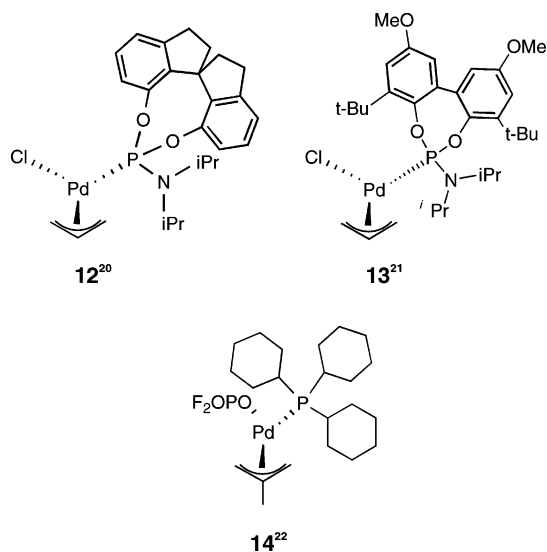
(22) Fernandez-Galan, R.; Manzano, B. R.; Otero, A.; Lanfranchi, M.; Pellinghelli, M. A. *Inorg. Chem.* **1994**, *33* (10), 2309.

(20) Shi, W.-J.; Xie, J.-H.; Zhou, Q.-L. *Tetrahedron: Asymmetry* **2005**, *16* (3), 705.

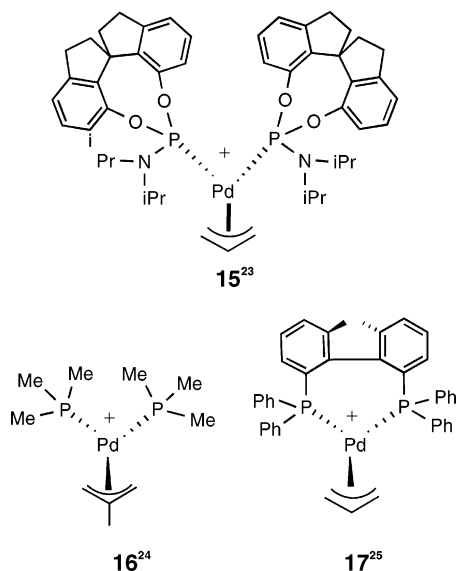
Table 1. X-ray Bond Distances (Å) and Angles (deg) for **4** and Several Model Allyl Complexes

	param	4 ^a	12 ²⁰	13 ²¹	14 ²²
	Pd(1)–C(1)	2.180(14)	2.222(4)	2.181(2)	2.208(8) 2.210(7)
	Pd(1)–C(2)	2.164(15)	2.141(4)	2.174(4) or 2.159(4)	2.150(7) 2.161(7)
	Pd(1)–C(3)	2.098(13)	2.097(4)	2.150(2)	2.085(8) 2.095(8)
	Pd(1)–P(1)	2.262(3)	2.2464(19)	2.296(1)	2.317(2) 2.314(2)
	Pd(1)–Cl(1)	2.392(3)	2.370(2)	2.360(1)	
	P(1)–Pd(1)–Cl(1)	101.8(1)	97.24(6)	96.83(2)	94.3(2) 94.6(2)
<hr/>					
	param	15 ²³	16 ²⁴	17 ²⁵	
	Pd(1)–C(1)	2.18(1)	2.178(6)	2.198(07)	
	Pd(1)–C(2)	2.19(1)	2.205(6)	2.181(18) or 2.160(18)	
	Pd(1)–C(3)	2.22(1)	2.189(7)	2.215(10)	
	Pd(1)–P(2)	2.296(2)	2.299(1)	2.304(02)	
	Pd(1)–P(1)	2.309(2)	2.299(1)	2.316(02)	
	P(2)–Pd(1)–P(1)	101.11(7)	100.2(1)	95.7(1)	

^a There are two independent molecules in the unit cell. However the geometrical parameters do not differ significantly ($\leq 3\sigma$); therefore only the bond distances and angles for one of the two independent molecules are reported in the table.

**Figure 2.** Ball-and-stick representation of the cation in **9**.

deal. In any case, the phosphoramidite *P-trans*-influence is stronger than the N atom of bipyridine in [Pd(bipy)(η^3 -CH₂C-



(Me)CH₂]⁺, **18**²⁶ (not shown in the table, Pd–Cl ca. 2.10 Å). Returning to **4**, we note that the Pd–Cl bond length is modestly long, ca. 2.39 Å, and the Cl–Pd–P angle, ca. 102°, rather large. We attribute both of these observations to the relatively large bulk of complexed **1**. The Pd–P distance in **4** is fairly normal, relative to the model complexes.²⁷

NMR Studies. ³¹P NMR data for the phosphoramidite species are given in Table 2. We also include the ³¹P data for the readily prepared dichloro complex PdCl₂(**1**)₂, **18**. The allyl chloro complexes **4**, **5**, **7**, and **8** reveal two ³¹P resonances for the two isomeric Pd complexes, which are assigned to structures involv-

(23) Shi, W.-J.; Xie, J.-H.; Zhou, Q.-L. *Tetrahedron: Asymmetry* **2005**, *16* (3), 705.

(24) Ozawa, F.; Son, T. I.; Ebina, S.; Osakada, K.; Yamamoto, A. *Organometallics* **1992**, *11* (1), 171.

(25) Knierzinger, A.; Schoenholze, P. *Helv. Chim. Acta* **1992**, *75* (4), 1211.

(26) Albinati, A.; Kunz, R. W.; Ammann, C. J.; Pregosin, P. S. *Organometallics* **1991**, *10*, 1800–1806.

(27) Orpen, A. G.; Brammer, L.; Allen, F. H.; Kennard, O.; Watson, D. G.; Taylor, R. *J. Chem. Soc., Dalton Trans.* **1989**, S1–S83.

Table 2. ^{31}P NMR Chemical Shift Data^a for the Ligands and Pd-Allyl Complexes

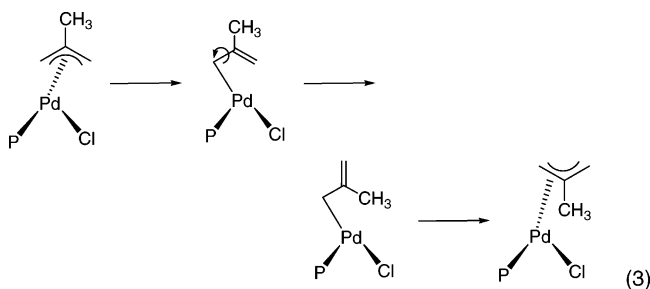
complex	major isomer (a)	minor isomer (b)
1	151.1	
2	142.1	
4	149.0	150.6
5	148.8	151.7
7	141.3	146.8
8	140.5	143.8
9	147.4, 148.0	
10	145.4, 145.8	
11	144.5, 145.1	
18	117.1	

^a $^2J(\text{P,P}) = 100.5$ Hz for **9**, 99.8 Hz for **10**, and 100.0 Hz for **11**. 700 MHz, CD_2Cl_2 .

ing different positions of the allyl ligands with respect to the asymmetric phosphoramidite. The relative populations for these isomers are ca. 2.2:1, 1.5:1, 1.5:1, and 1.3:1 for **4**, **5**, **7**, and **8**, respectively. Their ^{13}C NMR spectra reveal that the terminal allyl carbon signals within each pair of isomers have similar chemical shifts (see Figure 3 and Tables 3 and S1), although those for the 2-methallyl species **4** and **5** are, as expected from the literature,^{28,29} somewhat different from those for the 1,3-diphenylallyl analogues **7** and **8** (see Table S2).

Generally, the ^1H NMR spectra of our phosphoramidite complexes appeared somewhat complicated; however, all of the important allyl and phosphoramidite resonances for both isomers were well resolved at 700 MHz in dichloromethane solution. Given the increasing use of phosphoramidite ligands, we have made an effort to assign the phosphoramidite ^1H and ^{13}C signals and give a representative selection of these in Tables 3 and 4. Further extensive NMR lists are given in the Supporting Information.

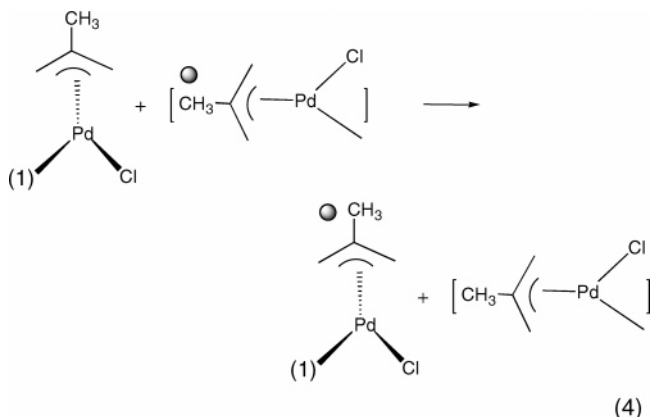
Phase-sensitive ^1H NOESY NMR spectra show selective cross-peaks due to exchange between the two isomers (see Figures 4 and 5 for representative examples). Interestingly, analysis of the exchange pathway, e.g., for **4**, reveals that *only one* methylene allyl set of protons, that *cis* to the phosphoramidite ligand, undergoes a *syn/anti* exchange process. These results are consistent with an $\eta^3\text{-}\eta^1$ allyl isomerization due to opening of the allyl under electronic control; that is, the stronger P-donor labilizes the *trans* position. This isomerization process is followed by a rotation of the vinylic group about the C–C bond.



Complexation to give the η^3 -allyl form affords the second isomer; see eq 3. In this mechanism *syn/anti* exchange is limited to the methylene group *cis* to the P-donor. This type of specific isomerization mechanism in chiral complexes has been reported previously.^{12,13}

In the synthesis of, for example, **4** and **5**, a slight excess of dinuclear complex $[\text{Pd}(\mu\text{-Cl})(\eta^3\text{-CH}_2\text{C}(\text{Me})\text{CH}_2)]_2$, **3**, is normally employed, so as to avoid the formation of the bis-phosphoramidite salts. When compound **3** is present in solution, the 2-D exchange map shows that it is *exchanging with the two*

isomers of **4** or **5** (see Figure 4). In eq 4, the gray ball is meant



as an indicator of the source of the allyl). The same kinds of cross-peaks are found in the 2-D NOESY maps for solutions of, for example, **7**, containing a small amount of $[\text{Pd}(\mu\text{-Cl})(\eta^3\text{-PhCHCHCHPh})]_2$, **6** (see Figure 6).

We initially considered that this exchange might arise due to dissociation of the phosphoramidite followed by attack of this now free ligand on the excess bridged starting material. However several experiments suggest that this is not correct: (a) a CD_2Cl_2 solution containing 1 equiv each of **4** and **7** (and no **3**) *did not reveal any cross-exchange*, but did show the usual intramolecular isomerization cross-peaks; (b) addition of a small amount of, for example, phosphoramidite **1** to a CD_2Cl_2 solution of **4** rapidly affords the bis-phosphoramidite **9**. Consequently, in the presence of free **1**, the bis-phosphoramidite forms from the chloro species **4** (see Figure 7); and (c) addition of a small amount of bridged starting material, **3**, to the CD_2Cl_2 solution containing the pure complexes **4** and **7** immediately induces dynamic behavior, and this is nicely shown via ^{31}P NMR (see Figure 8). These results suggest that the chloro-bridged complex acts as a *reagent* to encourage the exchange reaction. Although we have no data in support of a mechanism, one can imagine that, for example, if a small amount of the unsaturated species “ $\text{PdCl}(\eta^3\text{-CH}_2\text{C}(\text{CH}_3)\text{CH}_2)$ ” were to form, it would readily complex the terminal halogen of **4**, which could then lead to allyl scrambling. Alternatively, an $\eta^1\text{-CH}_2\text{C}(\text{CH}_3)=\text{CH}_2$ fragment from **4** (see eq 3) might be able to use the double bond to cleave **3**, again with subsequent allyl scrambling. In any case, the observation that **3** *induces* an allyl exchange is both interesting and potentially relevant for the enantioselective allylic alkylation reaction.²¹ Any reagent that facilitates allyl face exchange could lead to changes in enantioselectivity.

As suggested in Figure 7, the ^{31}P NMR spectra for the bis-phosphoramidite complexes reveal two different ^{31}P spins and thus a (tightly coupled) AB spectrum as a consequence of the diastereotopic P atoms.³⁰ From a structural point of view this observation can be understood using the X-ray results shown in Figure 2. The two coordinated phosphoramidite ligands are not symmetrically placed with respect to the allyl ligand, and thus the two ^{31}P spins are nonequivalent. In solution there are *four* nonequivalent ^1H allyl chemical shifts in the 2-methallyl

(28) Åkermark, B.; Krakenberger, B.; Hansson, S.; Vitagliano, A. *Organometallics* **1987**, *6*, 620.

(29) Malet, R.; Moreno-Manas, M.; Pajuelo, F.; Parella, T.; Pleixats, R. *Magn. Reson. Chem.* **1997**, *35*, 227–236.

(30) A set of low-temperature ^{31}P spectra for **9** reveal (a) that the two resonances react differently to the decrease in temperature, with the result that several classical AB patterns are observed and (b) there is a temperature dependence of the line shape in that one resonance broadens faster than the other (see the Supporting Information).

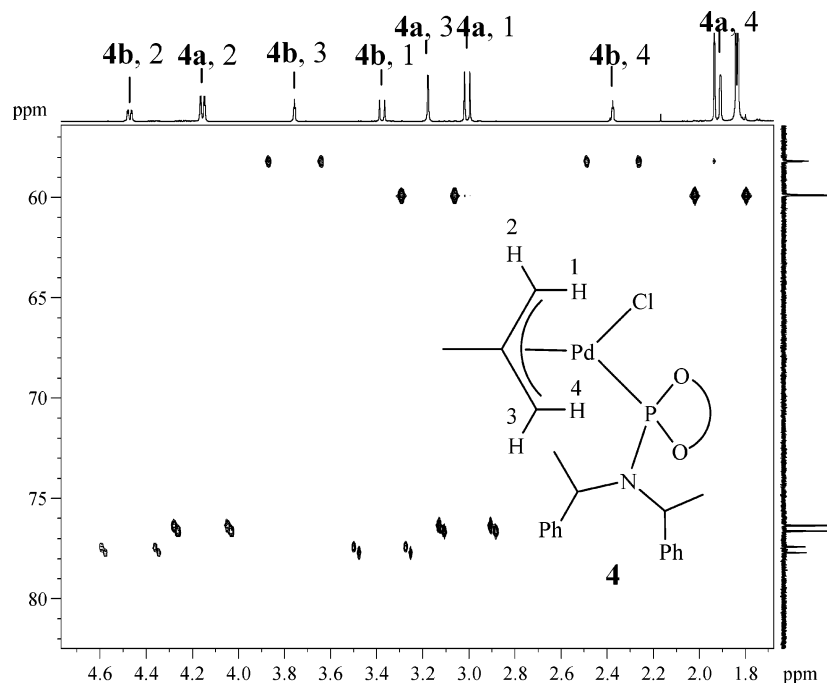
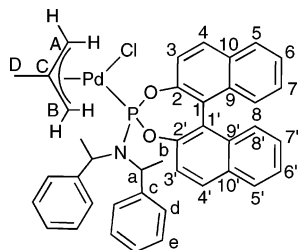


Figure 3. Section of the one-bond $^{13}\text{C}, ^1\text{H}$ correlation NMR spectrum for **4**, revealing the cross-peaks for the two terminal allyl carbons of the two isomers. The cross-peaks associated with the allyl C atom *trans* to Cl are found at ca. 60 ppm, whereas those *trans* to the P atom are located at ca. 75 ppm (CD_2Cl_2 , 700 MHz).

Table 3. The ^1H and ^{13}C NMR Chemical Shift Data^a for the Isomers of the Allyl Complex **4**



site	^1H		^{13}C	
	a	b	a	b
A	<i>anti</i> 3.00 <i>syn</i> 4.16	<i>anti</i> 3.38 <i>syn</i> 4.47	77.0	78.1
B	<i>anti</i> 1.91 <i>syn</i> 3.18	<i>anti</i> 2.38 <i>syn</i> 3.76	60.5	58.7
C			133.3	133.8
D	1.02	1.93	22.4	22.3
a	4.89	5.09	55.3	55.3
b	1.84	1.55	21.7	21.7
c			141.6	141.4
d	7.44	7.22	128.8	128.4
e	7.32	7.18	127.9	127.6
2			148.7	148.2
3	7.98	8.07	123.9	123.3
4	8.01	8.07	130.2	130.4
5	7.99	7.94	128.2	128.3
6	7.49	7.45		
2'			149.7	149.2
3'	8.03	8.03		
4'	7.44	7.22		

^a 700 MHz, in CD_2Cl_2 .

complexes, thereby confirming that the two complexed P-donors afford a chiral pocket in which the “left” and “right” sides are different. The ^{13}C allyl chemical shifts, given in Table 3, reflect the presence of two (as opposed to one in, for example, **4**) P-donors. The analogous 2-D exchange spectroscopy (for **9** and **10**) shows that there is *no* exchange between the nonequivalent P-donors.

Concluding, it would seem that the mono- and bis-phosphoramidite allyl complexes do not demonstrate similar exchange patterns. However, with respect to an allyl ligand, both the mono- and bis-phosphoramidite Pd complexes create asymmetric environments. The presence of excess dinuclear allyl complex **3** promotes an allyl exchange reaction.

Experimental Part

All reactions and manipulations were performed under an N_2 atmosphere using standard Schlenk techniques. Solvents were dried and distilled under standard procedures and stored under nitrogen. NMR spectra were recorded with Bruker DPX-250, 300, 500, and (mostly) 700 MHz spectrometers at room temperature. Chemical shifts are given in ppm; coupling constants (J) in hertz. Elemental analyses and mass spectroscopic studies were performed at the ETHZ.

o,o'-(*S*)-(1,1'-Dinaphthyl-2,2'-diyl)-*N,N'*-di-(*S,S*)-1-phenylethylphosphoramidite (**1**) and *o,o'*-(*S*)-(1,1'-dinaphthyl-2,2'-diyl)-*N*-benzyl-*N*'-(*S*)-1-phenylethylphosphoramidite (**2**) have been synthesized according to the literature.³¹

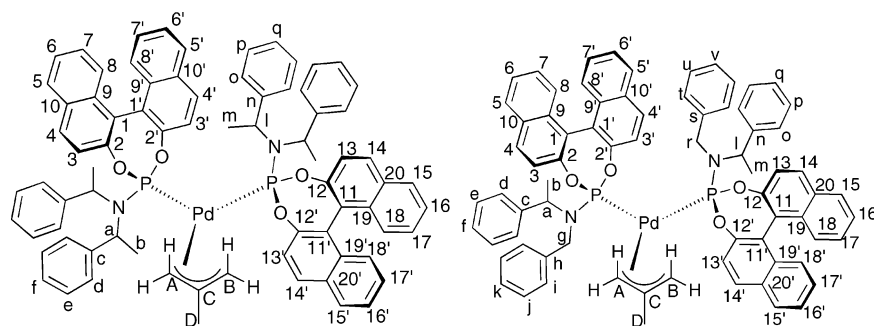
Crystallography. Air-stable, colorless crystals of **4** were obtained by crystallization from diethyl ether/ CH_2Cl_2 solution. A crystal of **4** was mounted on a Bruker SMART diffractometer, equipped with a CCD detector for the data collection. The non-centrosymmetric space group was chosen due to the presence of a chiral ligand; the cell constants were refined at the end of the data collection with the data reduction software SAINT.³² The experimental conditions for the data collections and crystallographic and other relevant data are listed in Table 5 and in the Supporting Information.

The collected intensities were corrected for Lorentz and polarization factors³² and empirically for absorption using the SADABS program.³³ The structure was solved by direct and Fourier methods and refined by full matrix least-squares,³⁴ minimizing the function

(31) Arnold, L. A.; Imbos, R.; Mandoli, A.; de Vries, A. H. M.; Naasz, R.; Feringa, B. L. *Tetrahedron* **2000**, *56*, 2865.

(32) BrukerAXS, SAINT, Integration Software; Bruker Analytical X-ray Systems: Madison, WI, 1995.

(33) Sheldrick, G. M. SADABS, Program for Absorption Correction; University of Göttingen: Göttingen, Germany, 1996.

Table 4. ^1H and ^{13}C NMR Chemical Shift Data^a for Complexes 9 and 10

site	9		10	
	^1H	^{13}C	^1H	^{13}C
A	<i>anti</i> 2.91 <i>syn</i> 4.31	72.8	<i>anti</i> 3.31 <i>syn</i> 4.86	72.6
B	<i>anti</i> 3.56 <i>syn</i> 4.39	70.9	<i>anti</i> 2.32 <i>syn</i> 4.87	73.8
C		141.8		141.2
D	2.06	23.8	1.49	21.9
a	4.80	55.1	4.51	55.8
b	1.20	20.4	1.05	18.9
c		141.6		139.7
d	6.49	127.3	6.77	127.2
e	7.01		6.93	127.0
f	7.14		7.10	125.2
g			3.57, 3.57	47.3
h				138.2
i			6.67	127.6
j			7.09	
k			7.09	125.7
l	4.60	55.3	4.76	56.8
m	1.07	20.2	1.35	19.5
n		141.5		140.7
o	6.56	127.5	6.71	127.4
p	7.02		6.89	127.3
q			7.05	126.0
r			3.89, 4.06	47.7
s				138.6
t			6.85	127.7
u			7.06	
v			7.06	125.5
2		148.1		148.4
3	7.90	120.5	7.62	119.7
4	8.37	132.3	8.11	131.8
5	8.14	129.1	8.06	128.7
6	7.60		7.56	
7	7.34		7.34	
8	7.20		7.28	
2'		146.4		146.9
3'	7.27	121.5	7.74	121.1
4'	8.11	131.8	8.18	131.4
5'	7.80	128.5	7.99	128.4
6'	7.25		7.50	
7'	7.04		7.31	
12		148.5		148.1
13	7.88	120.4	7.78	119.7
14	8.34	132.3	8.28	132.2
15	8.12	129.1	8.15	128.8
16	7.57		7.61	
17	7.31		7.38	
18	7.15		7.31	
12'		146.2		146.6
13'	7.01	120.5	7.48	120.4
14'	7.93	131.8	7.91	131.3
15'	7.68		7.87	128.6
16'	7.26		7.53	
17'	7.11		7.33	

^a 700 MHz, in CD_2Cl_2 .

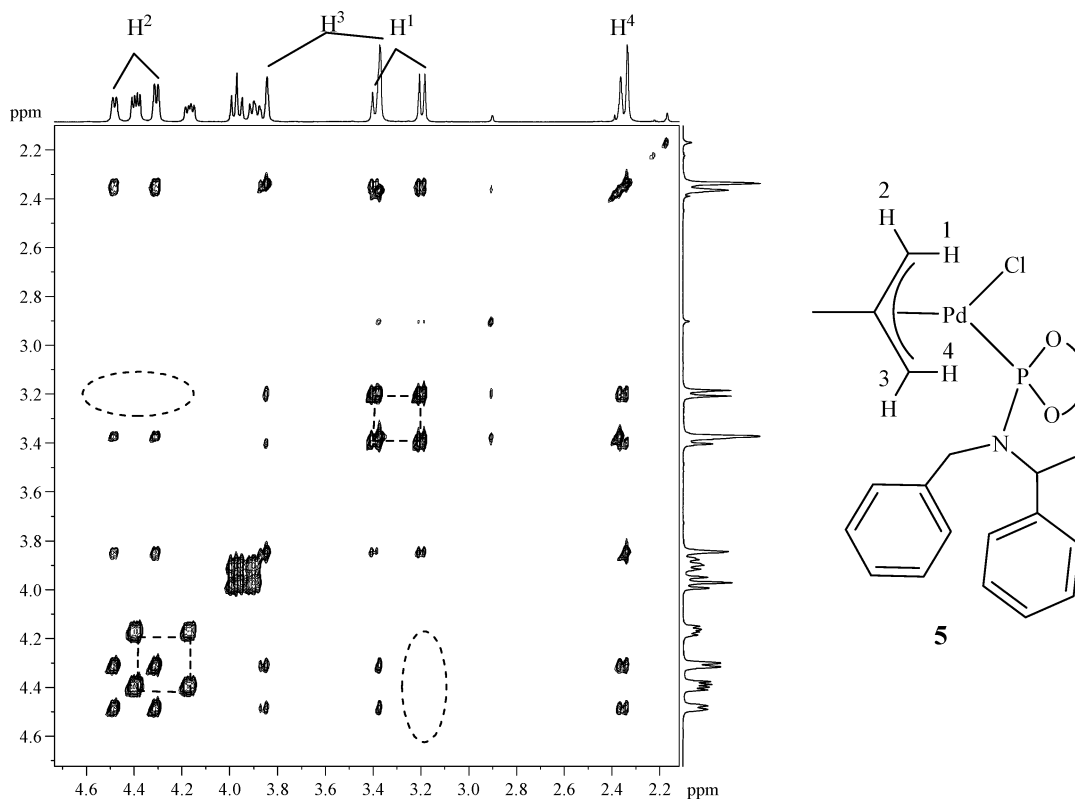


Figure 4. Section of the exchange NMR spectrum for **5**, showing the cross-peaks for the allyl protons H¹–H⁴ and those for the aliphatic methylene signals (not numbered). The exchange between the two isomers is visible in several places, e.g., (center) for the two H¹ protons and (lower left) for one of the aliphatic methylene resonances. The dotted circle indicates that H¹ does not exchange with H²; that is, there is no *syn/anti* exchange (CD₂Cl₂, 700 MHz).

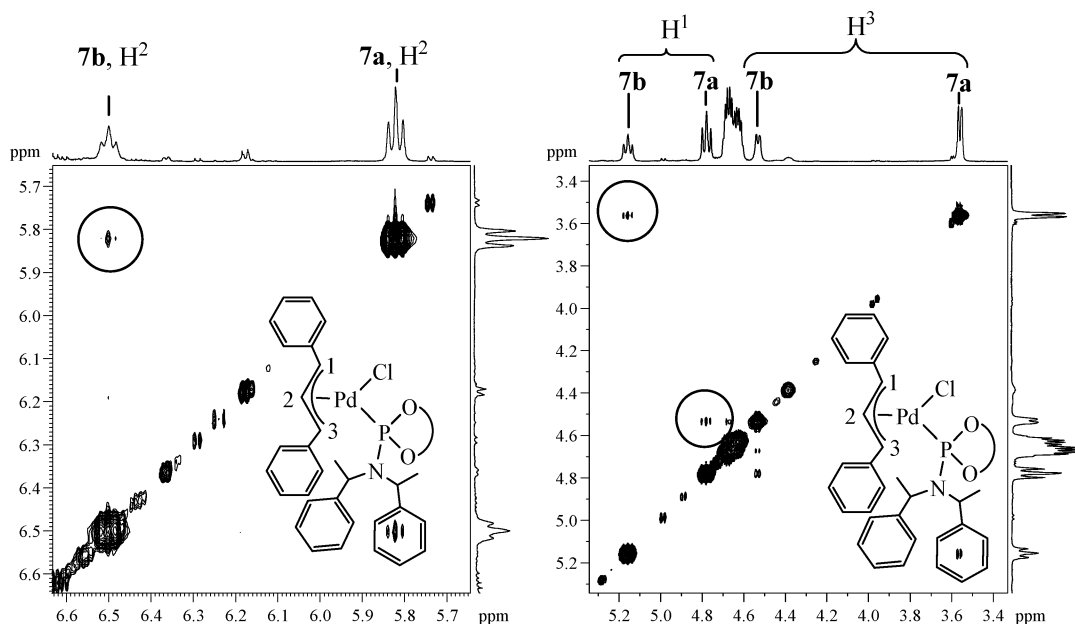


Figure 5. Sections of the exchange NMR spectrum for **7**, showing (left) the cross-peaks for the exchange involving the allyl proton H² and (right) the specific exchange of H¹ in **7a** and H³ in **7b**. The phenyl moieties (lower right in both) surround several cross-peaks (CD₂Cl₂, 700 MHz).

$[\sum w(F_o^2 - (1/k)F_c^2)^2]$ and using anisotropic displacement parameters for the Pt, P, N, and O atoms and for the C atoms of the allyl moieties. No extinction correction was deemed necessary. The contribution of the hydrogen atoms (except those of the clathrated water molecules) in their calculated position was included in the refinement using a riding model ($B(\text{H}) = aB(\text{C}_{\text{bonded}})$ (Å²), where a

= 1.4 for the hydrogen atoms of the methyl groups and $a = 1.2$ for the others).

The quality of the crystals was unsatisfactory, a fact that, together with positional disorder of the water molecules, led to poor agreement factors at the end of the refinement; however, upon convergence, the final Fourier difference map showed no significant peaks. The scattering factors used, corrected for the real and imaginary parts of the anomalous dispersion, were taken from the literature.³⁵

(34) Sheldrick, G. M. *SHELX-97, Structure Solution and Refinement Package*; Universität Göttingen, 1997.

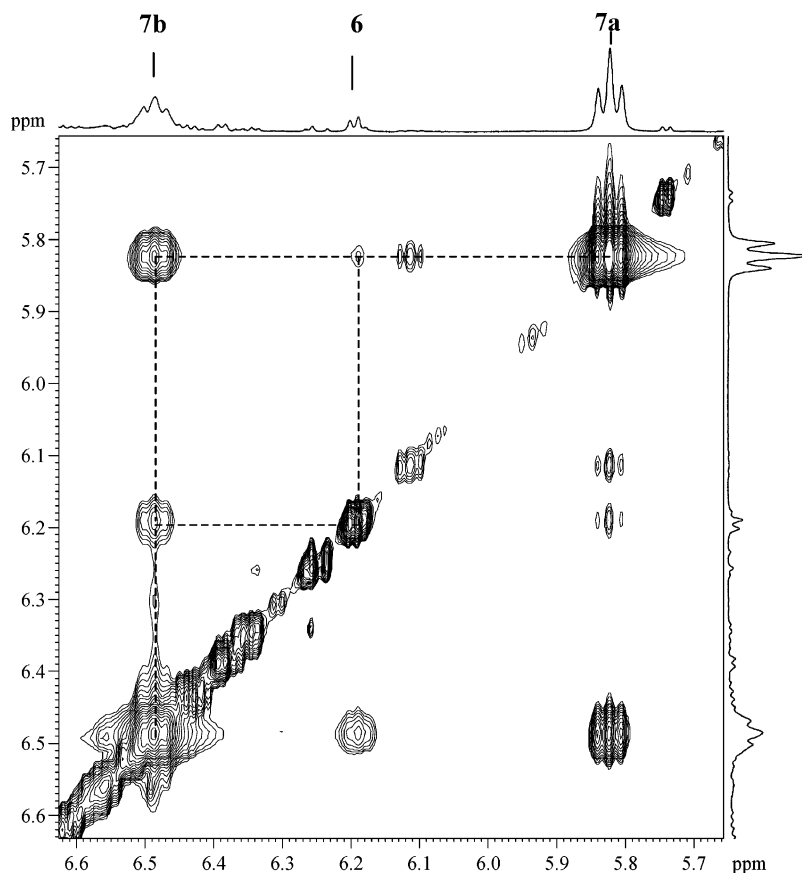


Figure 6. Section of the exchange NMR spectrum for complex **7**, in the region of proton H², showing the cross-peaks for the exchange involving the dinuclear complex **6** with the isomers of **7**. Note that (a) one of the two isomers affords more intense cross-peaks and (b) there are additional exchange pathways that, presumably, stem from exchange involving *syn/anti* isomers (CD₂Cl₂, 700 MHz).

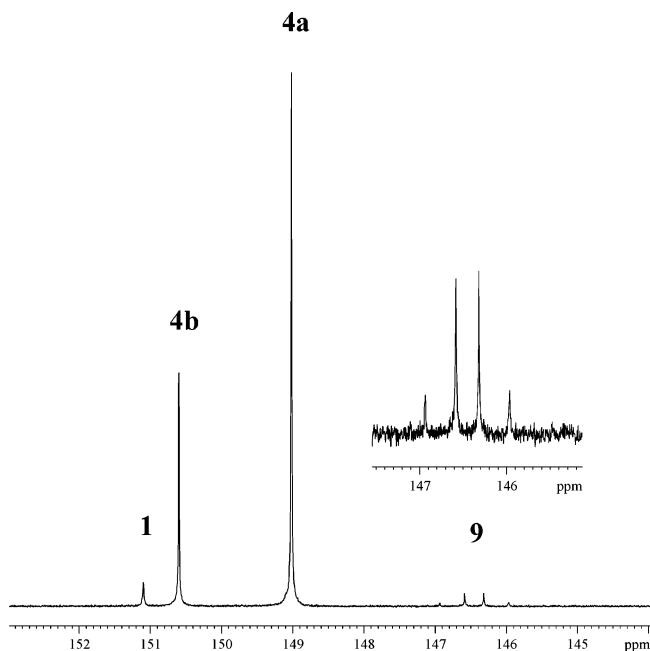


Figure 7. ³¹P NMR spectrum for a solution of **4** to which a small amount of free ligand **1** has been added. The bis-phosphoramidite AB spin system for complex **7** is readily observed (CD₂Cl₂, 700 MHz).

The standard deviations on intensities were calculated in terms of statistics alone. All calculations were carried out by using the PC version of the programs WINGX,³⁶ SHELX-97,³⁴ and ORTEP.³⁷

Synthesis of [PdCl(allyl)(phosphoramidite)]. A solution of the P-donor ligand (0.180 mmol, 2.0 equiv) in CH₂Cl₂ (5 mL) is slowly

added, under stirring, to a solution of the suitable dinuclear species [Pd(μ-Cl)(allyl)]₂ (0.090 mmol, 1.0 equiv) in CH₂Cl₂ (5 mL). After the addition is finished, the solution is stirred for 15 min, then the solvent is removed under reduced pressure, giving a solid, which is washed with diethyl ether and dried under vacuum.

[PdCl(CH₂C(CH₃)CH₂)(1)] (4): yellowish-white solid, yield 95%. Crystals suitable for X-ray were obtained by layering diethyl ether in a CH₂Cl₂ solution of the isolated complex. Anal. Calcd for C₄₀H₃₇ClNO₂PPd: C, 65.23; H, 5.06; N, 1.90. Found: C, 64.42; H, 5.16; N, 1.90. MALDI MS: 700 (M⁺ - Cl), 644 (M⁺ - Cl - CH₂C(CH₃)CH₂), 538 (M⁺ - Cl - CH₂C(CH₃)CH₂ - Pd).

[PdCl(CH₂C(CH₃)CH₂)(2)] (5): white solid, yield 94%. Anal. Calcd for C₃₉H₃₅ClNO₂PPd·H₂O: C, 63.25; H, 4.76; N, 1.89. Found: C, 62.31; H, 4.85; N, 1.93. MALDI MS: 686 (M⁺ - Cl), 526 (M⁺ - Cl - CH₂C(CH₃)CH₂ - Pd).

[PdCl(PhCHCHCHPh)(1)] (7): yellow solid, yield 91%. Anal. Calcd for C₅₁H₄₃ClNO₂PPd: C, 70.03; H, 4.95; N, 1.60. Found: C, 69.74; H, 5.15; N, 1.56. MALDI MS: 838 (M⁺ - Cl), 644 (M⁺ - Cl - PhCHCHCHPh), 538 (M⁺ - Cl - PhCHCHCHPh - Pd).

[PdCl(PhCHCHCHPh)(2)] (8): yellow solid, yield 92%. Anal. Calcd for C₅₀H₄₁ClNO₂PPd·H₂O: C, 68.34; H, 4.93; N, 1.59. Found: C, 67.91; H, 4.73; N, 1.62. MALDI MS: 1054 (M⁺ + PhCHCHCHPh), 824 (M⁺ - Cl), 630 (M⁺ - Cl - PhCHCHCHPh), 524 (M⁺ - Cl - PhCHCHCHPh - Pd).

Synthesis of [Pd(allyl)(phosphoramidite)]₂BF₄. A solution of the P-donor ligand (0.180 mmol, 4.0 equiv) in CH₂Cl₂ (5 mL) is added, under stirring, to a solution of the suitable dinuclear species

(35) *International Tables for X-ray Crystallography*; Wilson, A. J. C., Ed.; Kluwer Academic Publisher: Dordrecht, The Netherlands, 1992; Vol. C.

(36) Farrugia, L. J. *J. Appl. Crystallogr.* **1999**, *32*, 837.

(37) Farrugia, L. J. *J. Appl. Crystallogr.* **1997**, *30*, 565.

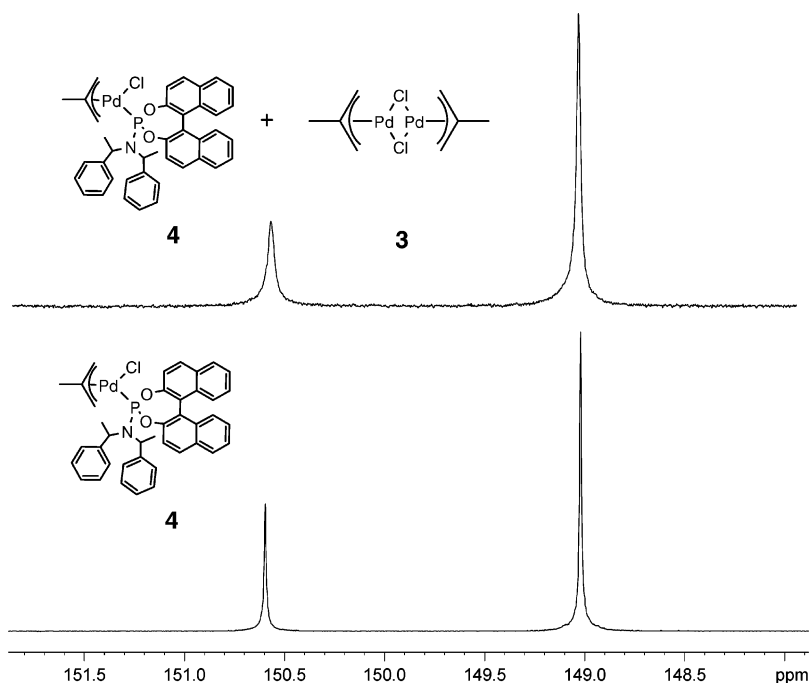


Figure 8. ^{31}P NMR spectrum of (a) a solution containing the isomers of **4** (lower trace) and (b) the same solution plus a small amount of dinuclear complex **3** (CD_2Cl_2 , 700 MHz).

Table 5. Experimental Data for the X-ray Diffraction Study of Compound 4

formula	$\text{C}_{80}\text{H}_{92}\text{Cl}_2\text{N}_2\text{O}_{12}\text{P}_2\text{Pd}_2$
mol wt	1615.17
data collection <i>T</i> , K	293(2)
diffractometer	Bruker SMART CCD
cryst syst	triclinic
space group (no.)	<i>P</i> 1 (1)
<i>a</i> , Å	9.710(3)
<i>b</i> , Å	13.593(4)
<i>c</i> , Å	15.154(5)
α , deg	85.181(8)
β , deg	89.777(8)
γ , deg	77.530(8)
<i>V</i> , Å ³	1945(1)
<i>Z</i>	2
ρ_{calcd} , g cm ⁻³	1.368
μ , mm ⁻¹	0.632
radiation	Mo $K\alpha$ (graphite monochrom $\lambda = 0.71073$ Å)
θ range, deg	$1.96 < \theta < 25.16$
no. data collected	16 316
no. indep data	13 490
no. obsd reflns (<i>n</i> _o)	10 212
$[F_o ^2 > 2.0\sigma(F ^2)]$	
no. of params refined (<i>n</i> _v)	496
<i>R</i> _{int}	0.0558
<i>R</i> (obsd reflns) ^a	0.0913
<i>R</i> (all reflns) ^a	0.1182
GOF ^b	1.046
abs struct param (Flack's param)	0.03(4)

$$^a R = \frac{\sum(|F_o - (1/k)F_c|)}{\sum|F_o|}. R_w^2 = \frac{[\sum w(F_o^2 - (1/k)F_c^2)^2 / \sum w|F_o|^2]}{[\sum w(F_o^2 - (1/k)F_c^2)^2 / (n_o - n_v)]^{1/2}}.$$

(0.045 mmol, 1.0 equiv) in CH_2Cl_2 (5 mL), followed by addition of a suspension of AgBF_4 (0.108 mmol, 2.4 equiv) in THF (5 mL). A precipitate forms immediately. The suspension is stirred for 45 min, after which time the solid is filtered. The resulting solution is concentrated under reduced pressure to a volume of 0.5 mL, and diethyl ether added to precipitate the product, which is then washed with diethyl ether and dried under vacuum.

[PdCl(CH₂C(CH₃)CH₂)(1)₂]BF₄ (9): light yellow solid, yield 92%. Crystals were obtained by layering diethyl ether in a CH_2Cl_2 solution of the isolated complex. Anal. Calcd for $\text{C}_{76}\text{H}_{67}\text{BF}_4\text{N}_2\text{O}_4\text{P}_2$ -

$\text{Pd}\cdot\text{CH}_2\text{Cl}_2$: C, 65.47; H, 4.92; N, 1.98. Found: C, 64.58; H, 5.09; N, 1.89. MALDI MS: 1187 ($\text{M}^+ - \text{CH}_2\text{C}(\text{CH}_3)\text{CH}_2$), 700 ($\text{M}^+ - \text{1}$), 644 ($\text{M}^+ - \text{CH}_2\text{C}(\text{CH}_3)\text{CH}_2 - \text{1}$), 540 ($\text{M}^+ - \text{CH}_2\text{C}(\text{CH}_3)\text{CH}_2 - \text{Cl} - \text{1} - \text{Pd}$).

[PdCl(CH₂C(CH₃)CH₂)(2)]BF₄ (10): light yellow solid, yield 93%. The microanalytical data are poor, presumably due to the tendency to absorb water; however, the NMR spectra are quite clear. MALDI MS: 1265 ($\text{M}^+ - \text{CH}_2\text{C}(\text{CH}_3)\text{CH}_2 + \text{Ag}$), 1159 ($\text{M}^+ - \text{CH}_2\text{C}(\text{CH}_3)\text{CH}_2$), 1054 ($2^+ + 2$), 686 ($\text{M}^+ - \text{Cl} - 2$), 632 ($\text{M}^+ - \text{CH}_2\text{C}(\text{CH}_3)\text{CH}_2 - \text{Cl} - 2$), 524 ($\text{M}^+ - \text{CH}_2\text{C}(\text{CH}_3)\text{CH}_2 - \text{Cl} - 2 - \text{Pd}$).

[PdCl(CH₂C(CH₃)CH₂)(Monophos)]BF₄ (11): whitish solid, yield 90%. The microanalytical data are poor, presumably due to the tendency to absorb water; however, the NMR spectra are quite clear. MALDI MS: 883 (M^+), 524 ($\text{M}^+ - \text{Monophos}$), 475 ($\text{M}^+ - \text{Monophos} - \text{CH}_2\text{C}(\text{CH}_3)\text{CH}_2$).

Synthesis of [PdCl₂(phosphoramidite)₂]. To a solution of $[\text{PdCl}_2(\text{PhCN})_2]$ (0.090 mmol, 1.0 equiv) in CH_2Cl_2 (5 mL) is added dropwise a solution of the suitable P-donor ligand (0.185 mmol, 2.05 equiv) in CH_2Cl_2 (5 mL). The solution is stirred for 15 min, then the solvent is evaporated under reduced pressure and the solid obtained is washed twice with diethyl ether.

[PdCl₂(1)₂] (18): yellow-orange solid, yield 96%. Crystals were obtained by layering diethyl ether in a CH_2Cl_2 solution of the isolated complex. Anal. Calcd for $\text{C}_{72}\text{H}_{60}\text{N}_2\text{O}_4\text{P}_2\text{Cl}_2\text{Pd}\cdot\text{H}_2\text{O}$: C, 67.85; H, 4.90; N, 2.20. Found: C, 67.66; H, 4.82; N, 2.34. MALDI MS: 1219 ($\text{M}^+ - \text{Cl}$), 1183 ($\text{M}^+ - 2\text{Cl}$), 644 ($\text{M}^+ - 2\text{Cl} - \text{1}$), 548 ($\text{M}^+ - \text{Cl} - \text{1} - \text{Pd}$).

Acknowledgment. P.S.P. thanks the Swiss National Science Foundation and the ETH Zurich for support, as well as the Johnson Matthey Company for the loan of palladium salts. We also thank Stefan Gruber for valuable help in the synthesis of the complexes.

Supporting Information Available: CIF files for the structure of **4**, tables of NMR data, and a variable-temperature ^{31}P NMR spectrum for **9**. This material is available free of charge via the Internet at <http://pubs.acs.org>.

OM060726P